The influence of the spot welding parameters on the quality of the jointing of two metal blanks HX300LAD+Z140MB

Nițu Mihai Cătălin, Șchiopu Adriana-Gabriela, Iordache Daniela Monica
National University of Science and Technology POLITEHNICA Bucharest Faculty of Mechanics and Technology

*Corresponding author: mihai.nitu_038@student.upit.ro

Abstract: Regarding the continuing concern about the environmental impact of carbon emissions and fossil fuel consumption, the reduction of the total mass of cars without compromising mechanical and structural performance, it proved to be an important factor. Thus, the joining of sheets in the automotive industry by the method of spot welding has grown, being an ideal choice in terms of high operating speeds, default of high production volume and high degree of automation. The delivery of parts to the customer at the required quality conditions implies the optimization of the main welding parameters in the process, following the recommendations for their establishment. The paper presents the influence of the parameters of the spot welding process: intensity, welding time, pressing force on the quality of the jointing of two HX300LAD + Z140MB blanks.

Keywords: welding parameters, core, jointing, quality

1. Introduction

In recent years, the, the continuing concern over the environmental impact of carbon emissions and fossil fuel consumption has led to a trend towards a decrease in the fuel consumption of passenger cars with a direct effect on reducing the quantity of polluting emissions, the increase in the number of travelled kilometers. At the same time, it was noted that an important factor in reducing fuel consumption is the decrease in the total mass of the car, which is, without compromising the mechanical and structural performance of the materials that make up the assembly, maintaining, according to standards, the impact resistance [1].

This led to the development of special high-strength steels with properties superior to ordinary steels. Thus, this superior strength allows designers to develop sheet metal parts with lower thickness, while still maintaining the mechanical strength of the assembly, being used in the basic structure of cars, being protected from the action of external factors by galvanization [2].

The most common method of joining sheets in the automotive industry is electric spot welding (SEP)[2], being an ideal choice, given the low production costs, high operating speeds and the readiness for automation. However, it also has some disadvantages represented by the fact that in the case of production lines with high volume and fast pace, the process may present disruptive factors such as electrode wear and tear, contamination of the surface of the workpiece [3].

The SEP process involves a cumulation of influences between electromagnetic, mechanical, fluid flow and metallurgical phenomena, being difficult to control because the final quality of the weld is determined by the interaction of several factors related to the process parameters along with the mechanical and electrical characteristics of the equipment [4]. It is materialized by obtaining a joint, which is directly influenced by the most important parameters of the process, namely the welding current (I – kA), clamping force between the electrodes (P – daN), welding time (Weld Time – cycles), and cooling temperature in the installation (°C) [1].

This paper presents a micro and macroscopic analysis of the test specimens obtained by spot welding. For both cases are presented the means and methods that helped to carry out the analysis, as well as the work mode that concluded in identifying the influence of the main parameters on the welding core. Following this, it was concluded on the choice of a set of parameters suitable for the type of material used, for obtaining quality welded assembly.
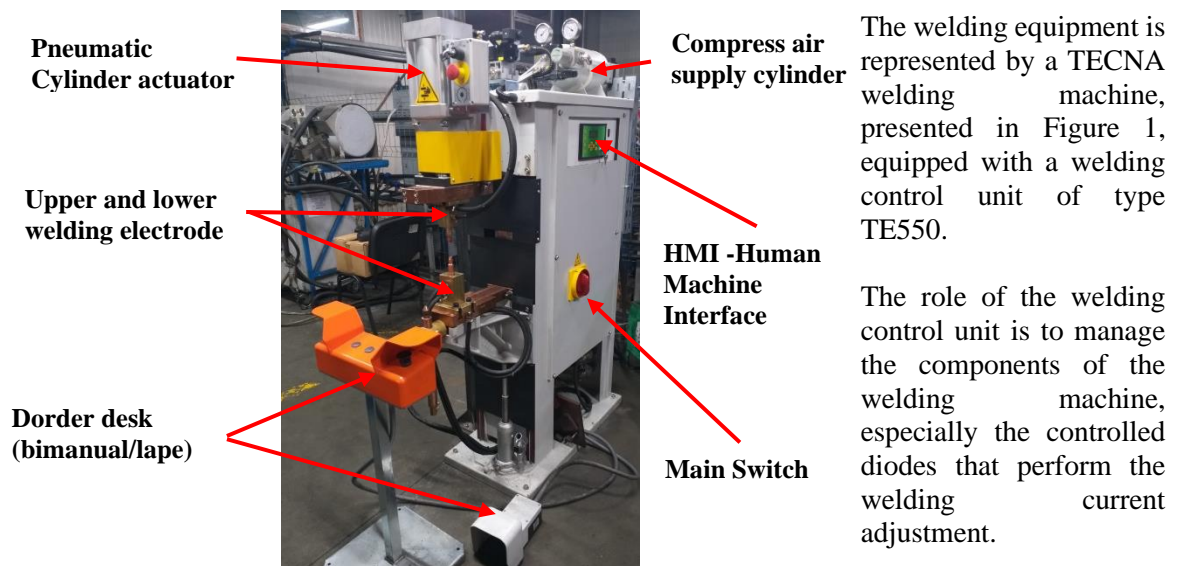
2. Experimental setup

Figure 1. Equipment used at SEP

The welding equipment is represented by a TECNA welding machine, presented in Figure 1, equipped with a welding control unit of type TE550.

The role of the welding control unit is to manage the components of the welding machine, especially the controlled diodes that perform the welding current adjustment.

The basic principle is the application of a heat to the surface of two materials to be joined, figure 2, following 3 phases:

- Heating at austenitizing temperature
- Diffusion (Keeping electrodes in contact)
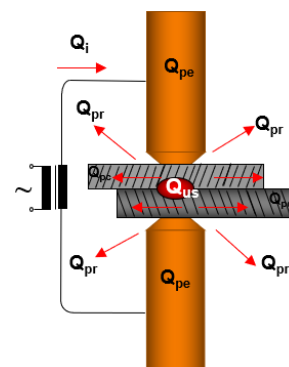- Recrystallization [5].

Figure 2. Thermal balance [6]

To perform the test the sheet metal samples are obtained by cutting from plate metal at dimensions 90 x 30 x 1,2 at quality HX300LAD + Z140MB, without passivation, figure 3. The sheet is covered with a layer of zinc with a thickness of 143 g/m2. According to Chan KR`s research [7] we can conclude the fact that at the electric pressure welding of galvanized sheets, the outer layer of zinc considerably decreases the weldability. More, Hamidinejad SM [8] in his work, he stated that the release of molten metal together with the premature wear of the contact surface of the electrodes is much more pronounced in the case of welding galvanized sheets than when welding sheets from classic steel.
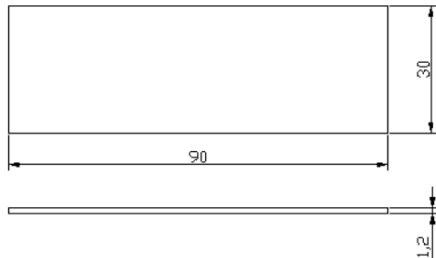

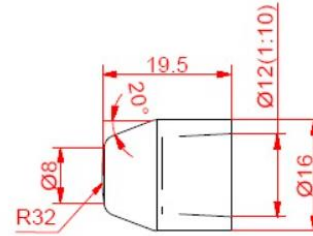**Figure 3.** Shape and dimensions of the samples

Figure 4. Shape and dimensions of the electrodes

The fact that the sheet does not have passivation reveals that it is not covered by that non-reactive layer with a thickness of a few atoms, which provides protection against the action of corrosive factors such as oxygen, water or chlorine ions.

After the chemical analysis of the sheet, the following concentrations of the elements are found, Table 1:

Table 1. Chemical composition of the welding material

C [%]	Si [%]	Mn [%]	P [%]	S [%]	Al [%]	Cu [%]	Ti [%]	Nb [%]
0,069	0,010	0,608	0,009	0,0074	0,049	0,014	0,001	0,011

The mechanical properties of this material are shown in Table 2 below:

Table 2. Mechanical properties of the welding material

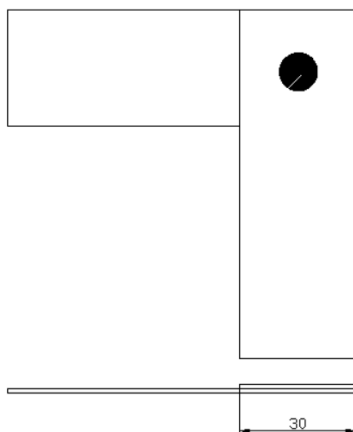| Tensile strenght [MPa]	Limit of elasticity [MPa]	Elongation [%]
300	402	34.3

Figure 5. Samples assemply

Following the adjustment of the above-mentioned parameters, the type of electrode necessary for welding the blanks is according to the chosen norms. Thus, G-type electrodes with the shape and dimensions shown in Figure 4 are used. The material of electrodes is CuCr1Zr – 2.1293 – CW106C. This is a high-strength material used for spot welding applications, suitable for most types of steel, including alloyed and stainless steel but also galvanized sheets, figure 5.

Following the microscopic analysis, it was observed that the central area of the joint is more concentrated in the case of the electrode with a radius at the tip, which leads to increased resistance to breaking [9].

One of the main parameters that will vary in the performance of the experiment is the pressing force of the upper electrode, P. The value of this force is influenced by the air flow that enters the pneumatic cylinder. This flow is adjusted manually by means of the air regulator on the entrance to the pneumatic route. The pressure value, in bar, is then read on the manometer. The pressure force measurement of the upper electrode is performed using the TECNA transducer, WeldTester model. For the second stage,

corresponding to the macroscopic analysis, the following means were used: microscope for TOOLCRAFT macroscopy and ZEISS AXIOVERT 200Mmat microscope.

3. Experimental results and disscusion

As regards the experimental results, in Table 3, the data extracted from the welding of samples, are presented, data to be interpreted from the point of view of the macroscopic and microscopic analysis of the welded core.

Table 3. Design of Experiments

No.	Intensity (kA)	Weld time (periods)	Pressing force (daN)	Joint area F (mm²)		
1	10,5	4,5	550	Sample 1	Sample 2	Sample 3
				17,2	17,08	18,34
2	11,8	4,5	390	Sample 4	Sample 5	Sample 6
				13,64	15,45	13,67
3	10,5	6	390	Sample 7	Sample 8	Sample 9
				16,96	17,16	17,43
4	11,8	6	550	Sample 10	Sample 11	Sample 12
				17,21	17,51	17,95

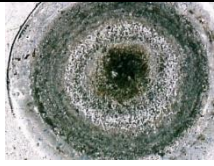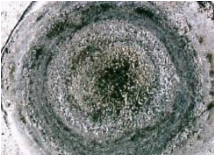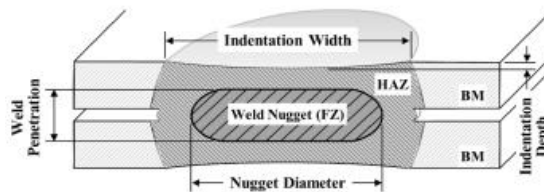The quality of the joint is measured by its diameter, figure 6:

Figure 6. Quality check of the welding point [10].

Macrographic Analysis. Following the macrographic analysis, the images were taken, using a 1.3M resolution (389 pixels), as shown in table 4. These highlight the influence of welding parameters on the appearance of the joint.

Table 4 Macrographic Analysis

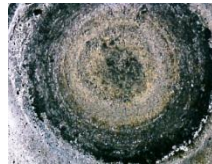| Sample No.	Appearance	Observation
1		In the transition zone is observed a limit of zinc + blended steel. The core is emphasized as an effect of the new electrode profile.
2		Analogous to piece 1, traces of molten zinc are observed towards the core.

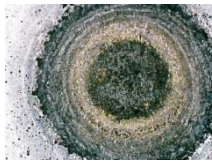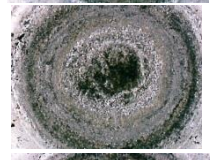|		
3		*The molten core is not clearly idealized because of the zinc coating.*
4		*A small core and a very large area of molten zinc are observed.*
5		*The black spot identifies the molten core, the current penetrating the zinc layer.*
6		*Analogous to piece 4 it is seen, through the yellowish stain, the molten zinc from top layer.*
7		*The current pierced the zinc layer and formed the core of molten steel.*
8		*The joint is formed, but the zinc layer is not completely pierced.*
9		*The boundaries of the joint are observed but it includes the top layer of zinc.*
10		*In the transition zone between the joint and Z.I.T. a good homogeneity is observed.*
11		*A sharp penetration may be observed due to the high current value. The obtained joint is conformed.*
12		*A sharp penetration can be observed due to the high current value. The obtained joint is conformed.*

Microscopic Analysis. This analysis consists in observing the microstructure of the melted material, both from the core area and the thermally influenced area, as well as from the areas bordering the welding point to the base material. The magnification chosen for obtaining relevant images was 100x. From the microscopic analysis, following the micrographs of the first 4 welded assemblies, the following conclusions can be drawn:

Sample no.1 is represented by the first specimen in the sample of set 1 corresponding to I = 10,5 kA; T = 4,5 periods; P = 550 daN. For a complete characterization 3 micrographs were taken as shown in Figure 7.
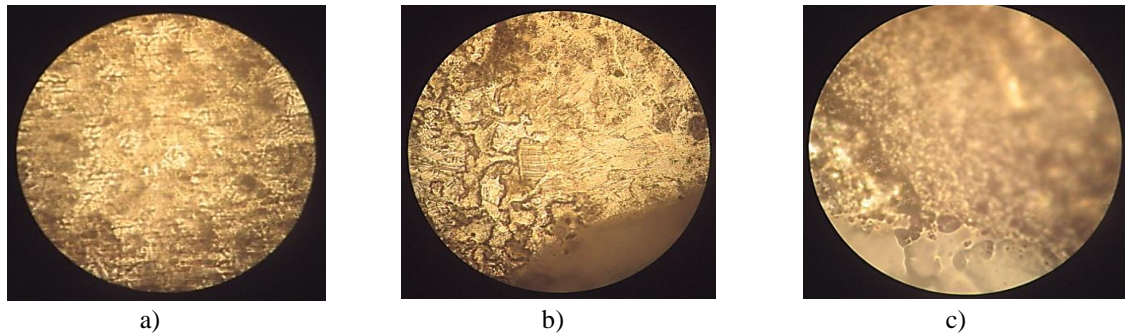

Figure 7. Microscopic analysis sample no. 1 (100X)

Figure 7 a) shows a microstructure of the base material with zinc coating over steel. The blurred image is caused by plastic deformation in the weld core area (the light is not perpendicular to the observation surface). In figure b) the micrograph approaches the core and larger sized zinc grains are represented, as an effect of the influence of temperature in the structure of the material. In figure c) is illustrated the maximum outside area of the welding core – heat-influenced area Qu, dispersed in Qpc. It is noted that apparently, the zinc grains shrink, the effect is reduced with the movement to the neighboring areas of the core.

Sample no.4 it is represented by the first specimen in the sample of the set 2 samples corresponding to I = 11,8 kA; T = 4,5 periods; P = 390 daN. At the microscopic analysis, 6 micrographs were taken as shown in Figure 8.
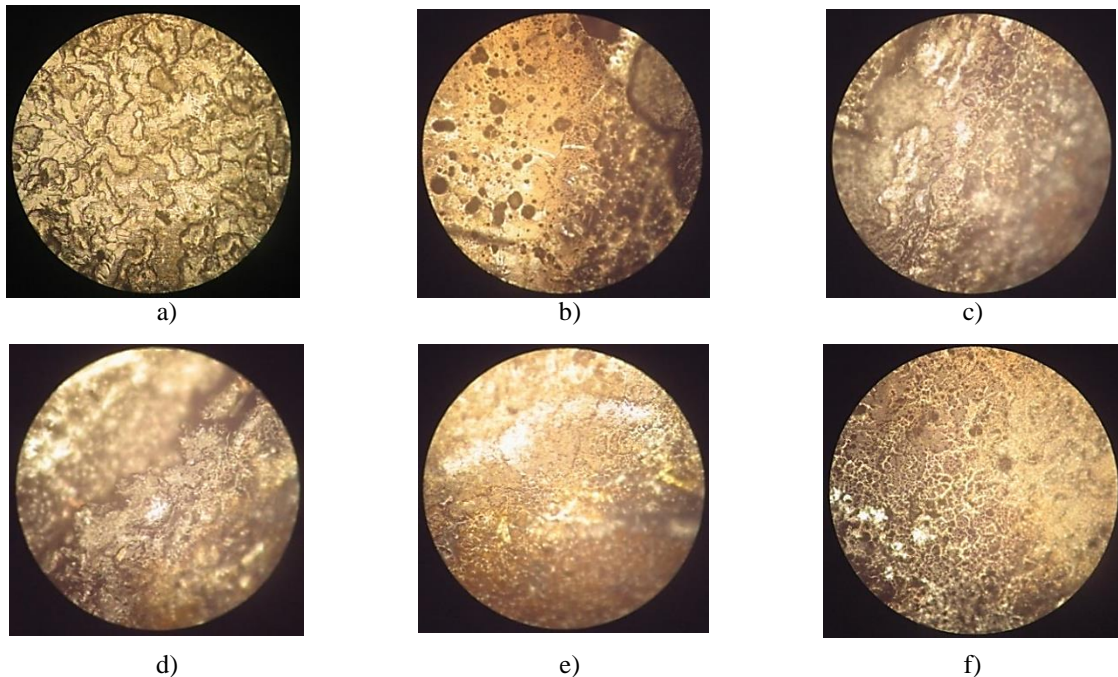

Figure 8. Microscopic analysis sample no. 4 (100X)

Figure 8 a) analogously illustrates the microstructure of the outer layer of zinc on the base piece, represented by zinc dendrites. Figure b) shows the starting zone of the thermally influenced area, on the left side, and on the right side is shown the area of the molten core. Figure c) presents the maximum boundary area of the molten core. Figure d) illustrates the microstructure of the molten material at the core. Homogeneity is observed between the border area and the center. At the same time a large grain size is observed, because of a small welding time, which does not provide a high resistance to stress and shocks. Figure e) shows a transition zone of yellowish tone between the thermally influenced area

(bottom area) and the base material (upper area). This shade is represented by the layer of partially molten zinc. From figure f) simultaneously perceive the three main areas of the welded assembly – core (starting from the left), thermally influenced area (middle) and base material.

Sample no.7 it is represented by the first specimen in the sample from the set 3 of samples corresponding to I=10,5 kA; T = 6 periods; P = 390 daN. At the microscopic analysis, 5 images were taken as shown in Figure 9.

a)   b)   c)
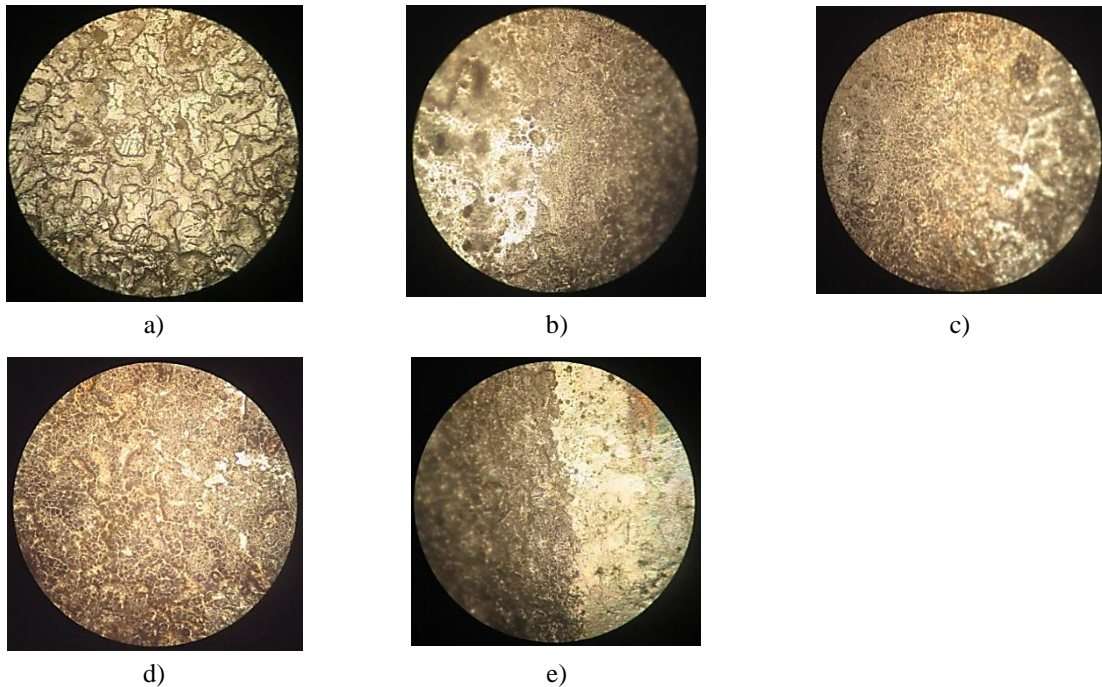

d)   e)

Figure 9. Microscopic analysis sample no. 7 (100X)

In figure 9 a) the zinc layer is represented in dendritic form. Figure b) shows the transition between the thermally influenced area and the joint. It can be observed smaller grains, as the effect of a longer welding time, as well, so a slow cooling by which the homogeneity of the molten material increases with effect in achieving a high hardness of the welded core and good resistance to mechanical stress and shock. Image c) shows a mixture of the base material, steel, with the coating material, zinc, resulting in a molten core of high quality. The yellowish shade is given by the external layer of melted zinc. The higher current value facilitated the mixture of the 2 materials. Figure d) illustrates the transition zone between the joint and the thermally influenced area from left to right.

From image e) information can be extracted related to the difference of the microstructure of the thermally influenced area compared to the area of the core material. In the thermally influenced area, an elongation of the microstructure grain is observed because of dispersion of the resulting heat.

Sample no.10 it is represented by the first specimen in the sample of the set 4 samples corresponding to I=11,8 kA; T = 6 periods; P = 550 daN. At the microscopic analysis were taken 5 images as in Figure 10.
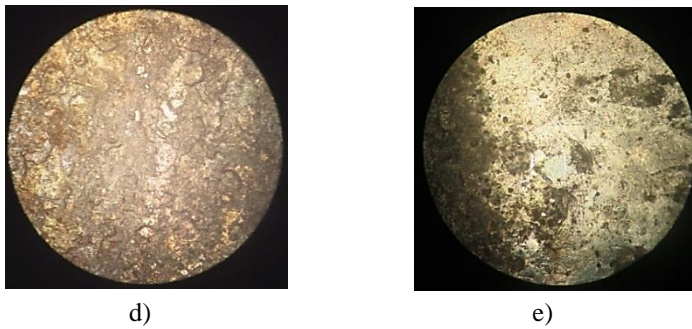

a)   b)   c)

| d) | e) |
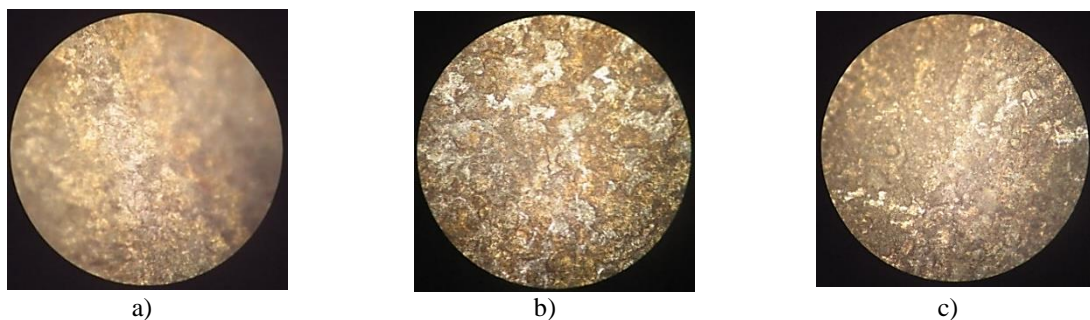
Figure 10. Microscopic analysis sample no. 10 (100X)

The first image, figure a) illustrates in the form of a structure in strips, the basic material with zinc coating. The structure is due to the plastic deformation of the blank obtained after lowering the upper package of the welding device. Figure b) shows melted zinc microstructures recognized by thermally affected yellowish grains. From figure c) a homogeneous transition zone between the melted zinc area and the thermally influenced zone is identified. Figure d) shows the melted core. It is noted that due to the high intensity of the current, the zinc layer was penetrated almost entirely, obtaining a welding core of molten steel of dark gray color. The last image e) illustrates the transition area towards the zinc layer of the core material.

4. Conclusion

From the scheme of welding equipment, we can state that among the main factors influencing the formation of the welding point is the secondary circuit.

The energy used to make the Qu welding is one of the components necessary for the realization of the welded core. At the same time, it is dissipated in the base material near the core, which is identified by the feeling of the high temperature near the joint, which can cause burns.

Also, the state of the welding surfaces influences the contact resistances between the electrodes and the parts. The higher these resistances, by the existence of deposits on the coating with oils or emulsions used in the production of base parts, the higher the chances of the appearance of burnt spots, pores on the surface, expulsions of molten material and reduction of the durability of electrodes.

In the case of microscopic analysis, the application of force greater than 390 daN and 550 daN, respectively, produces a plastic deformation of the welded core, results in a hollow shape, what at observation through the microscope affects the clarity of the image, obtaining an aberration at sphericality. This occurs because of deformation of the observation field.

From the previous we can settle that from the macro and microscopic analysis it resulted that for a conformal welding, without expulsion of material and a uniformity of molten material, correlated with the types of welded materials, the force applied by the electrode during welding has an important role. Sufficient value is required to enable structural transformations to occur throughout the welded core area, to uniform the grain and to melt the base material and the coating together (ex. Steel + Zinc).

From the point of view of the optimal parameters, we can state that for welding 2 sheets of steel with a composition and properties similar to the one presented in the work, using the same type of electrode, we can say, type G, for high quality and high resistance to mechanical stress of the welding point, an intensity equal to 10.5 kA can be used, a welding time of 6 periods and a pressing force between 380 and 400 daN.

5. References

[1]   Rajarajan C, Sivaraj P, Sonar T, Raja S, Mathiazhagan N. Resistance spot welding of advanced high strength steel for fabrication of thin-walled automotive structural frames. Forces in Mechanics 2022;7. https://doi.org/10.1016/j.finmec.2022.100084.

[2]   DiGiovanni C, He L, Pistek U, Goodwin F, Biro E, Zhou NY. Role of spot weld electrode geometry on liquid metal embrittlement crack development. J Manuf Process 2020;49:1–9. https://doi.org/10.1016/j.jmapro.2019.11.015.

[3]   Dai W, Li D, Zheng Y, Wang D, Tang D, Wang H, et al. Online quality inspection of resistance spot welding for automotive production lines. J Manuf Syst 2022;63:354–69. https://doi.org/10.1016/j.jmsy.2022.04.008.

[4]   Zhou K, Yao P. Overview of recent advances of process analysis and quality control in resistance spot welding. Mech Syst Signal Process 2019;124:170–98. https://doi.org/10.1016/j.ymssp.2019.01.041.

[5]   Maurice A. Soudage par resistance 2002.

[6]   Curs Renault Caroserie Nepublicat. ACADEMIA AUTOMOBILULUI DACIA SUDAREA ELEMENTELOR DE CAROSERIE. 2008.

[7]   Chan KR, Scotchmer N, Zhao J, Zhou Y. Weldability Improvement Using Coated Electrodes for RSW of HDG Steel. 2005.

[8]   Hamidinejad SM, Kolahan F, Kokabi AH. The modeling and process analysis of resistance spot welding on galvanized steel sheets used in car body manufacturing. Mater Des 2012;34:759–67. https://doi.org/10.1016/j.matdes.2011.06.064.

[9]   Chen T, Ling Z, Wang M, Kong L. Effect of a slightly concave electrode on resistance spot welding of Q&P1180 steel. J Mater Process Technol 2020;285. https://doi.org/10.1016/j.jmatprotec.2020.116797.

[10]   Xia YJ, Zhou L, Shen Y, Wegner DM, Haselhuhn AS, Li YB, et al. Online measurement of weld penetration in robotic resistance spot welding using electrode displacement signals. Measurement (Lond) 2021;168. https://doi.org/10.1016/j.measurement.2020.108397.